Draft version February 14, 2025
Typeset using LaTeX **twocolumn** style in AASTeX631

Linking the Oscillation Profiles of δ Scuti Stars to Their Evolutionary Phases

Subrata Kumar Panda [1] and Shravan Hanasoge [1]

[1] *Department of Astronomy and Astrophysics, Tata Institute of Fundamental Research, Colaba, Mumbai 400005, Maharashtra, India*

ABSTRACT

Central environments of stars, which remain inaccessible to conventional observations, play crucial roles in determining their evolution stages. Oscillations, that propagate throughout the stellar interior and are measured at the surface, have the ability to probe the internal conditions. Here, we report how the oscillations of main-sequence intermediate-mass stars evolve in response to changes in their cores. As these stars evolve, the frequencies of their strongest (highest-amplitude) oscillation modes ($\nu_{\rm max}$) tend to decrease while their amplitudes ($A_{\rm max}$) increase. The second-strongest oscillation modes in most of the stars are found to have frequencies ranging from half to twice that of the $\nu_{\rm max}$, and their amplitudes are at least $0.1A_{\rm max}$. The range of frequencies over which the high-amplitude modes resonate are also found to systematically decrease with the extent of evolution. The correlations between the frequencies and amplitudes of the prominent oscillation modes in these stars may be useful for characterizing the evolutionary phases of intermediate mass stars. We also found a relationship between their $\Delta\nu$ and $\nu_{\rm max}$, making the latter a meaningful characteristic of δ Scuti stars.

1. INTRODUCTION

Stellar oscillations provide a means with which to examine (Aerts 2021) the internal functioning of stars, whose masses range from low (Brito & Lopes 2021) to high (Bowman 2020) and whose evolutionary phases stretch from the pre-main sequence (Zwintz & Steindl 2022) to white dwarf stage (Córsico 2020). Asteroseismology can supplement existing observational methods or techniques, allowing for investigation of a multitude of phenomena, ranging from star formation to Galactic archaeology. With the wealth of stellar pulsation data available from space observatories such as Kepler (Borucki et al. 2010), K2 (Howell et al. 2014), and TESS (Ricker et al. 2014), the study of stellar evolution using asteroseismology presents significant opportunities to advance many areas of stellar astrophysics.

While the oscillation characteristics of many stars across the HR diagram are well understood, the pulsations of intermediate-mass ($1.5-2.5M_{\odot}$) stars during their main sequences (the phase of core Hydrogen fusion) are challenging to interpret. Commonly termed as δ Scutis, these stars are hot objects of A-F spectral type (6000 K $\leq T_{\rm eff} \leq$ 9000 K; Uytterhoeven, K. et al. 2011) that can spin rapidly (Royer, F. et al. 2007) - upto several cycles per day - and vibrate on timescales of minutes-to-hours. The acoustic oscillations are driven by the κ (opacity) mechanism (Chevalier 1971; Baglin et al. 1973) originating in the He^+ plasma in their radiative envelopes. Unlike the orderly pulsation frequencies seen in other stars, rapid rotation and non-linear excitation processes in δ Scutis generate complex sequences of resonances.

δ Scutis oscillations (Bedding et al. 2020) during the phase that occurs shortly after the onset of Hydrogen fusion in their cores – a stage marked as zero-age main sequence (ZAMS) – are somewhat well understood. At this stage, their pulsation cavities are relatively simple in structure (Handler 2009). Subsequently, as the stars evolve, their pulsation cavities become increasingly complex, making them more challenging to identify. In the Terminal-Age Main Sequence, these stars evolve into red giants, and their oscillation profiles become amenable to interpretation by the asymptotic theory of stellar oscillations.

Here, we show that the pulsation profiles of the δ Scuti stars in general may be utilized to determine their phases of evolution. Investigating the spectral profiles of these stars in the order of their evolutionary hierarchy may capture the details regarding the emergence of mixed modes, and the complexity of δ-Scuti oscillations.

2. RESULT

We analyzed the δ Scuti stars available in Singh et al. 2025 (in preparation) computing various statistical properties of their acoustic oscillations. Table 1 makes these information available for all the stars. We also attempted to acquire their structure parameters from Gaia DR3 (Fouesneau, M. et al. 2023) inferred through the module *Final Luminosity Age Mass Esti-*

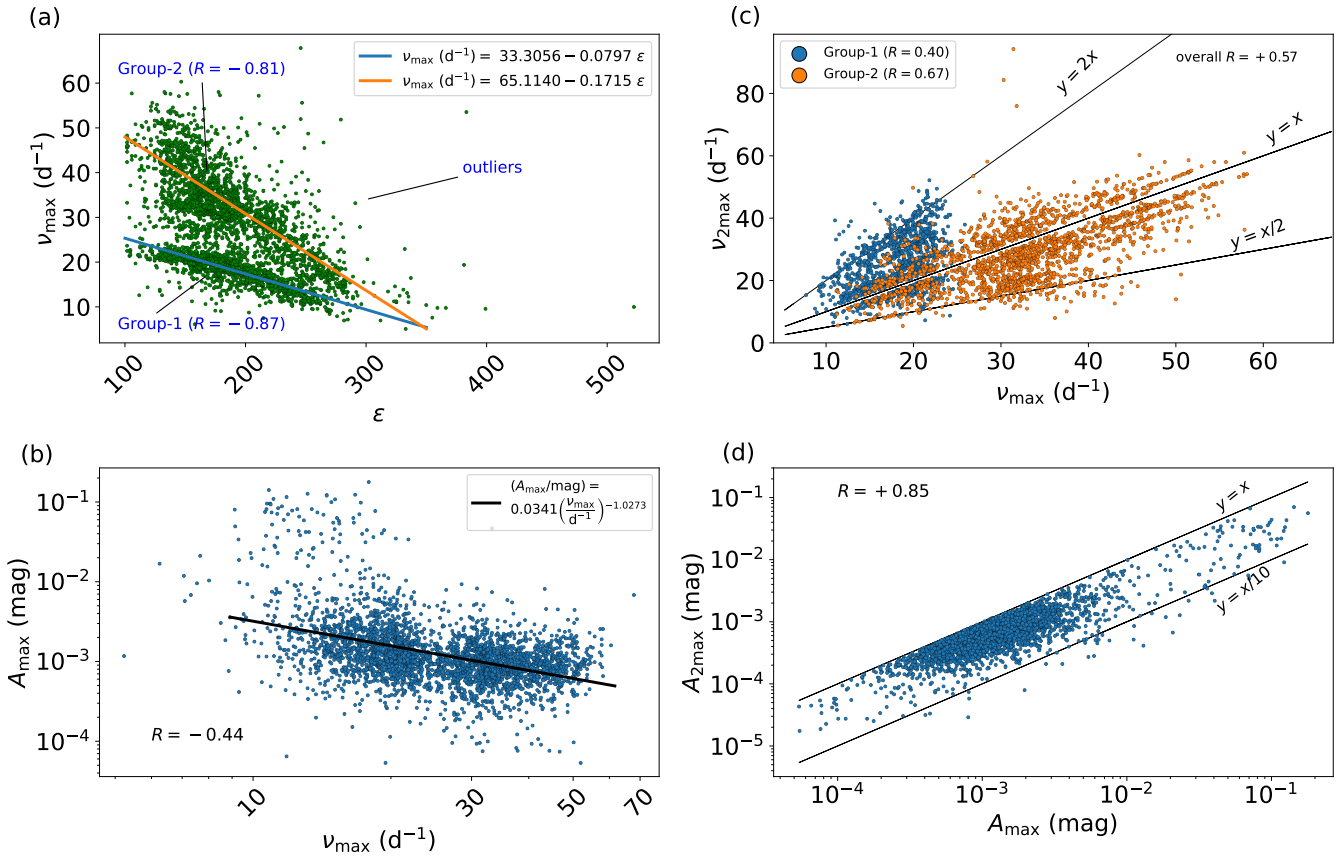

Figure 1. (a) ν_{max}, the frequency corresponding to the largest oscillation amplitude, gradually decreases as the stars evolve (left to right). The data appear to cluster densely in two regions. (b) Amplitude (A_{max}) inversely decreases as a function of frequency (ν_{max}). Both x- and y-axis are in logarithmic scale. (c) Frequency of the mode with the second largest amplitude, plotted against ν_{max}. In most δ Scutis, this frequency lies between $[0.5\nu_{max} - 2\nu_{max}]$. Stars are color coded according to the Groups into which they were classified (see Figure 1a). (d) Second-strongest amplitude (A_{2max}) plotted as a function of A_{max}. The former is correlated with the latter for most stars in our sample. Both x- and y-axes are in log scale.

mator (FLAME). These quantities have been computed by fitting BaSTI stellar evolution models (Hidalgo et al. 2018) to photometric and spectroscopic observations captured by Gaia. Two notable parameters of interest are the age (τ) and the evolutionary stage (ε). Evolutionary stages are closely tied to the core environments of stars, where nuclear reactions take place. Stars of identical ages can exist in different evolutionary phases if they have unequal masses, and hence varying rates of energy generation. It explains why some open clusters comprise both main sequence and red giants together (Mermilliod et al. 1998; Balona et al. 2012).

Gaia DR3 provides the evolutionary phases in the form of dimensionless integers which tag stars based on their internal compositions. Figure 4 and Table 4 of Hidalgo et al. (2018) demonstrate how the parameter ε is assigned to distinct evolutionary phases of various stars. While the zero-age main sequence (ZAMS) is marked with $\varepsilon = 100$, the terminal age main sequence (TAMS) is tagged by $\varepsilon = 420$, base of RGB by $\varepsilon = 490$, and the values of ε for all intermediate stages are interpolated in between these limits. Out of the initial sample of 6711 stars, we were finally left with nearly 3200 objects for which all the aforementioned quantities were simultaneously available.

2.1. *Evolution of the dominant frequency*

One of the asteroseismic properties we calculated was the frequency of the mode of the maximum amplitude (ν_{max}). It represents an important property of evolved stars such as red giants and solar-like stars, and is usually defined as the central frequency of the Gaussian-shaped envelopes of their pulsation amplitudes. It characterizes their frequency regularities (large separation, $\Delta\nu$) that eventually determine the frequencies of the other acoustic modes (Gough 1986). Although Gaussian-like amplitude envelopes are not commonly observed in δ Scuti spectra, their ν_{max} is identified as either the frequency of the highest amplitude (Balona

TIC	$\nu_{\rm max}$ (d^{-1})	$A_{\rm max}$ (mag)	$\nu_{\rm 2max}$ (d^{-1})	$A_{\rm 2max}$ (mag)	$f_{\rm low}$ (d^{-1})	$f_{\rm high}$ (d^{-1})	ϵ	age (Gyr)
336485998	6.2654	0.0169	12.5420	0.0082	6.2654	18.8162	158	0.5420
364399376	7.0775	0.0120	14.1560	0.0074	7.0775	25.2852	312	0.9540
144101735	7.1176	0.0058	14.3751	0.0024	7.1176	14.3371	282	1.0270
270265624	7.3334	0.0068	12.1662	0.0036	7.3334	14.6841	285	0.9940
–	–	–	–	–	–	–	–	–
32559046	58.0092	0.0007	54.2182	0.0006	39.4659	58.0092	133	0.3210
3965274	58.0438	0.0026	54.7268	0.0009	41.5362	58.0438	178	0.6690
461695820	60.3300	0.0016	56.3050	0.0003	51.6994	60.3300	147	0.4470
278048697	67.7952	0.0069	66.1026	0.0013	57.3507	69.0749	246	0.8900

Table 1. Various asteroseismic characteristics we calculated for about 3200 stars, along with their evolutionary parameters obtained from Gaia DR3. TIC refers to the ID of the stars according to the TESS Input Catalog. **The complete dataset is available in the online article.**

& Dziembowski 2011; Bedding et al. 2023) or the amplitude-weighted frequency average (Barceló Forteza et al. 2018). In this article, we examine the evolution of the two most significant modes and explore the potential information they can convey.

We found that $\nu_{\rm max}$ decreases as stars evolve (Figure 1a), similar to the declining trend found in case of red giants (Stello et al. 2016). As these stars evolve, they become larger in size, leading to increased sound-cross times for the resonant modes. Hence the oscillation period becomes longer, resulting in a reduction in the corresponding frequency. However, the appearance of two clusters in Figure 1(a) suggests that the $\nu_{\rm max}$ of these stars decreases along two distinct pathways, including a few instances that do not follow any structured trend. We used the Gaussian mixture model from `scikit-learn` (Pedregosa et al. 2011) to cluster these stars into two categories: Group-1 with lower $\nu_{\rm max}$ and Group-2 with relatively higher $\nu_{\rm max}$, along with the remaining stars classified as outliers. Group-1 consists of $\sim$ 36% stars of the entire sample, and Group-2 comprises $\sim$ 56%, and the outliers account for $\sim$ 6.8% of stars. Because this classification is based on density of points in the phase space, the algorithm separates the outliers which are far away from the dense regions of the domain. Thus the outliers shown in Figure 1 should not be treated as another Group of δ Scutis with distinct characteristics.

We observe an approximately linearly declining trend in $\nu_{\rm max}$ with evolutionary phase ε. The Pearson coefficient R, i.e., the linear correlation between the two quantities ε and $\nu_{\rm max}$, was found to be -0.87 for Group-1 and -0.81 for Group-2 stars. To quantify the correlations between these quantities, we fitted linear models to the individual Groups of data with MCMC and obtained the relations

$$\nu_{\rm max}/{\rm d}^{-1} = (-0.0797 \pm 0.0001)\varepsilon + (33.3058 \pm 0.0217)$$

for Group-1 stars, and

$$\nu_{\rm max}/{\rm d}^{-1} = (-0.1715 \pm 0.00008)\varepsilon + (65.1140 \pm 0.0164)$$

for stars in Group-2. It can be observed that stars belonging to Group-2 maintain their $\nu_{\rm max}$ at nearly twice that of the Group-1 stars. While $\nu_{\rm max}$ of Group-1 stars are relatively tightly constrained and gradually reduce with ε, $\nu_{\rm max}$ for Group-2 stars is spread over a wider frequency range and rapidly declines with evolutionary phase. The correlation between $\nu_{\rm max}$ and ε for Group-2 stars appears largely scattered, particularly at the younger evolutionary phases.

A similar dual-ridge structure is also observed in the period-luminosity ($P_{\rm max} - L$) diagrams of δ Scutis (Figure 1 of Ziaali et al. 2019, Figure 2 of Barac et al. 2022), with a ratio of two between the $P_{\rm max}$ values of the two ridges. Ziaali et al. (2019) identified the $P_{\rm max}$ of the primary group (the tighter ridge) of stars as being associated with fundamental radial modes (e.g., $n = 1, \ell = 0$). They proposed that the $P_{\rm max}$ of the stars in the secondary (diffuse) ridge may correspond to higher-order overtones, as this group comprises relatively hotter stars where the excitation mechanism can drive modes of higher n to attain the highest amplitudes. Barac et al. (2022) demonstrated that amplitude modulation (Bowman et al. 2016) in stars belonging to the

secondary ridge reduces the amplitudes of their fundamental modes and causes excitation of other modes to the highest amplitudes, thereby making mode identification challenging. Their explanation can also account for the two-ridge structure we observed in Figure 1(a).

In addition to the higher-overtone radial ($\ell = 0$) harmonics, the $\nu_{\rm max}$ of the Group-2 stars may also be identified as modes of non-radial ($\ell > 0$) nature, which are expected to be split by rotation into a set of $(2\ell + 1)$ multiplets, roughly separated by rotational frequency. Individual components of such multiplets can attain the strongest amplitude, and statistically, over ensemble scales, produce $\nu_{\rm max}$ whose spread is proportional to the rate of rotation. The amount of scatter associated with the $\nu_{\rm max}$ in our figure 1(a) exhibits a similar decreasing nature, in line with the rotational slow-down of stars as they evolve. The spread in rotation has been proposed by García Hernández et al. (2022) as a contributing factor to the broadening of the period-luminosity relation of δ Scuti stars.

2.2. *Evolution of the dominant amplitude*

The mechanisms through which oscillation modes gain their amplitudes in δ Scutis are not fully understood, whereas their frequencies are better constrained by theoretical models. Observed pulsation magnitudes are in general the result of convolution between the intrinsic mode amplitudes and the mode visibilities, which depend on mode geometry and the inclination angle of the rotation axis (Daszyńska-Daszkiewicz, J. et al. 2002; Reese, D. R. et al. 2013). Detailed non-linear calculations, which have yet to be explored (Balona 2024), are necessary to gain insights into the processes determining the intrinsic mode amplitudes. On top of all these factors, amplitude modulation adds another layer of complexity to the consistent determination of pulsation amplitudes (Bowman et al. 2016). However, a few systematic correlations have been observed between $A_{\rm max}$ (the amplitude of $\nu_{\rm max}$) and general observables, including the dependence with $v \sin i$ (Fig. 2 of Breger 1982, Fig. 14 of Gaia Collaboration et al. 2023), inclination angle (Fig. 3 of Suárez, J.-C. et al. 2002), and luminosity (Fig. 10 of Read et al. 2024). We primarily study the evolution of this amplitude and its correlation with potential asteroseismic parameters.

In Figure 1(b) we show the link between the amplitudes ($A_{\rm max}$) and frequencies ($\nu_{\rm max}$) of the strongest oscillation modes obtained from the spectrum of each δ Scuti star we analyzed. A weakly declining trend is observed. Assuming $A_{\rm max}$ follows a power law function of $\nu_{\rm max}$, we examined the linear correlation between $\log A_{\rm max}$ and $\log \nu_{\rm max}$, and obtained a Pearson correlation coefficient $R = -0.44$. The correlation is obscured by the large scatter, which may arise from the spread in rotation (García Hernández et al. 2022), inclination angle of the rotation axis, and visibility among many other factors. It should also be noted that amplitude in general is not a function of only frequency; instead it can also show a mass-metallicity dependence. Using MCMC, we fitted a linear model to these two quantities and obtained

$$\log A_{\rm max} = (-1.0273 \pm 0.065) \log \nu_{\rm max} - (1.4666 \pm 0.09),$$

which translates to

$$A_{\rm max} \approx 0.0341 \ \nu_{\rm max}^{-1.0273},$$

with $A_{\rm max}$ in magnitude and $\nu_{\rm max}$ in units of $\rm d^{-1}$.

This observation is intuitive when considering an elementary example of a simple harmonic oscillator, whose total energy is given by $E_{\rm total} = 0.5 m \omega^2 A^2$, where $\omega = 2\pi\nu$ is the angular frequency and A the amplitude. Under adiabatic conditions, where total energy is conserved, a decrease in the frequency must result in an inversely proportional rise in the amplitude. This principle applies to mechanical vibrations, including the sound (acoustic) wave that primarily determines δ Scuti oscillations. In this case, the mode kinetic energy E_k is given in the form of $A^2\nu^2$ (Barceló Forteza, S. et al. 2017), which thus implies $A \sim \nu^{-1}$. Our best-fit model $A_{\rm max} \propto \nu_{\rm max}^{-1.0273}$ aligns with this expectation, suggesting that changes in $\nu_{\rm max}$ primarily determine corresponding shifts in the intrinsic mode amplitude $A_{\rm max}$. Amplitude reduction with $\nu_{\rm max}$ has also been reported in red giants (Sreenivas et al. 2024). Even though δ Scutis pulsate in very different ways than the other groups of pulsators, a common principle appears to govern the evolution of the $\nu_{\rm max}$ and $A_{\rm max}$ in all these stars.

2.3. *Evolution of the second-dominant mode*

Although the nature of $\nu_{\rm max}$ and $A_{\rm max}$ have been investigated in detail, the properties of other modes are scarcely understood. Figure 6 of Hey, Daniel & Aerts, Conny (2024) visually suggests systematic relations between the frequencies of the dominant modes in δ Scuti stars. Here we study the characteristics of the modes having the second strongest amplitude. We identified these modes such that they are at least $1\rm d^{-1}$ away from $\nu_{\rm max}$ in order to avoid selecting side lobes of the strongest mode (which may occasionally exhibit the second largest amplitude). We label the amplitude and frequency of this mode as $A_{\rm 2max}$ and $\nu_{\rm 2max}$ for subsequent reference.

In Figure 1(c), we plot $\nu_{\rm 2max}$ against $\nu_{\rm max}$. The $\nu_{\rm 2max}$ of most of the stars are often confined between $\nu_{\rm max}/2$

and $2\nu_{\rm max}$. Two dense clusters appear in this diagram, which may be reconciled as stars belonging to Groups 1 and 2, marked in Figure 1(a). Group-1 stars occupy the region where $\nu_{\rm max} < 20{\rm d}^{-1}$ and their $\nu_{\rm 2max}$ consistently remains within the range of $[0.5\nu_{\rm max} - 2\nu_{\rm max}]$. In contrast, $\nu_{\rm max}$ of the Group-2 stars is spread across the entire range, with a notable prevalence in the region where $\nu_{\rm max} > 30{\rm d}^{-1}$. Although $\nu_{\rm 2max}$ of the Group-2 stars disperse within the range $[0.5\nu_{\rm max} - 2\nu_{\rm max}]$, they are preferably closer to $\nu_{\rm max}$ at younger ages (and hence larger $\nu_{\rm max}$), with the spread gradually increasing with evolution (or, decreasing $\nu_{\rm max}$). The apparent connection between $\nu_{\rm max}$ and $\nu_{\rm 2max}$, along with the factor 2 that constrains the permissible range of $\nu_{\rm 2max}$, suggests that the radial orders of the two strongest amplitude modes are related. Pearson coefficient R, which was measured to be +0.57 in this case, establishing a moderate correlation between $\nu_{\rm max}$ and $\nu_{\rm 2max}$.

Much as the frequencies of the two dominant oscillation modes, their amplitudes also appear to be correlated. We label the amplitude of the second strongest mode as $A_{\rm 2max}$ for subsequent reference. In Figure 1(d), we show the interdependence between $A_{\rm max}$ and $A_{\rm 2max}$. A Pearson correlation coefficient of $R = 0.85$ was obtained between these two quantities. $A_{\rm 2max}$ of a majority of stars appear at least above $1/10^{\rm th}$ of their $A_{\rm max}$. The $A_{\rm 2max}$ for a significant fraction of the sample is comparable to $A_{\rm max}$. Based on the correlations between $\nu_{\rm max} - \nu_{\rm 2max}$ and $A_{\rm max} - A_{\rm 2max}$ observed in Figure 1 (c and d), we speculate that the highest-amplitude mode plays an important role in determining mode frequencies as well as amplitudes of the neighboring radial orders.

2.4. *Evolution of other dominant modes*

Instead of further analyzing the properties of the modes with successive significance, we investigated the frequency ranges across which the stars pulsate with observable amplitudes. Because δ Scuti oscillations often exhibit modes with continuously varying amplitudes, distinguishing significant modes can be challenging. Here, we selected modes having a signal-to-noise ratio above 4, where signal refers to the mode amplitude and noise corresponds to the $95^{\rm th}$ percentile of the whole amplitude array. We obtained the minimum ($f_{\rm low}$) and maximum ($f_{\rm high}$) bounds of the frequencies of all stars and examined their correlations with stellar evolutionary stages, as shown in Figure 2(a). The pattern is dispersed, leading to $f_{\rm low}$ and $f_{\rm high}$ exhibiting lower degrees of correlations with ε, e.g., $R = -0.5$ and -0.57 respectively. Hence, we did not intend to perform a quantitative fit. Nevertheless, the diagonal shapes formed by the over-dense data points indicate that the frequency

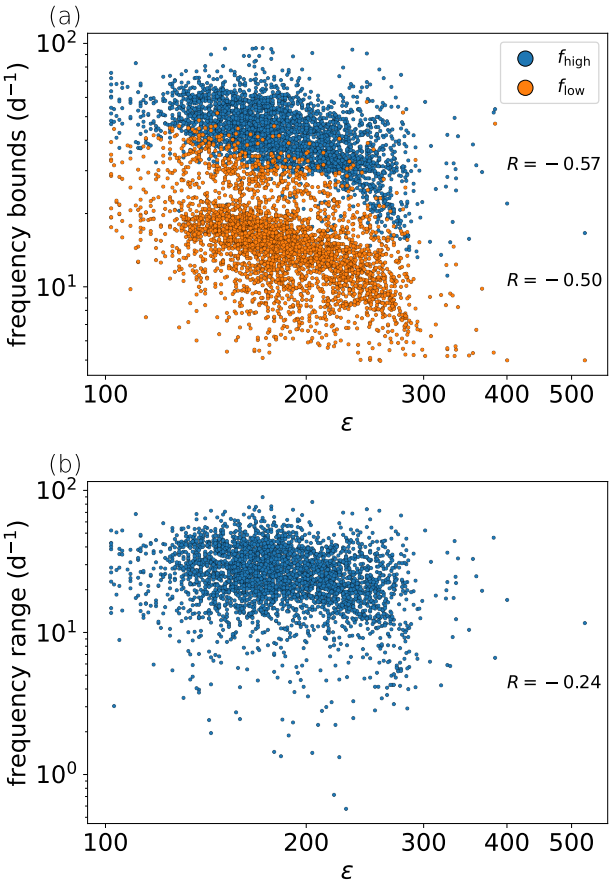

Figure 2. (a) Evolution of the lower as well as higher frequency bounds between which modes of significant amplitudes (signal-to-noise ratio > 4) are distributed. Much as the decrease in the characteristic frequency $\nu_{\rm max}$, these mode boundaries also shift downward in frequency as the stars evolve. (b) Frequency range, defined as the difference between the mode boundaries, is shown as a function of evolutionary stage ε. The frequency rage is approximately constant through various stages of evolution, as indicated from the weak correlation ($R = -0.24$) it exhibits with ε.

bounds gradually decrease with evolution. In Figure 2(b) we plot the frequency range ($\Delta f := f_{\rm high} - f_{\rm low}$) as a function of evolutionary stage ε. This quantity is nearly constant over these evolutionary stages during the main sequence. The low correlation coefficient of $R = -0.24$ between Δf and ε indicates the weak relationship between evolution and oscillation-frequency range.

2.5. *Connection with Large frequency separation*

Main-sequence oscillators - solar-like and red giants - pulsate in p-modes, uniformly spaced in frequency. This constant spacing is referred to as the large-frequency separation ($\Delta\nu$), and scales proportionally with $\nu_{\rm max}$.

However, because the oscillations of δ Scutis are driven by the κ mechanism, thereby complicating their interpretation, $\delta\nu$ can thus be measured in about 6% of the stars. A detailed discussion on the properties and definitions of $\nu_{\rm max}$ in δ Scutis can be found in Bedding et al. (2023). While Bedding et al. (2020) have measured $\Delta\nu$ of 60 δ Scuti stars, Singh et al. 2025 (in preparation) provide it for nearly 400 stars. We obtained $\nu_{\rm max}$ for these stars and examined whether they are connected to $\Delta\nu$.

In Figure 3 we plot $\Delta\nu$ as a function of $\nu_{\rm max}$, which shows scatter - as expected - and a correspondingly weak correlation coefficient $R = 0.38$. We distinguish the stars in this figure based on the Groups identified previously (Figure 1a). Stars in Group-1 appear to maintain a tight $\nu_{\rm max} - \Delta\nu$ relation, whereas stars in Group-2 show diffuse variations. For comparison's sake, we also show an empirical relation of type $\Delta\nu(\mathrm{d}^{-1}) = 0.4(\nu_{\rm max}/\mathrm{d}^{-1})^{0.77}$, similar to the characteristics of Solar-like pulsators such as sub-giants and Red giants. Although this relation aligns with the properties of a few targets, the overall $\Delta\nu - \nu_{\rm max}$ dependence in the δ Scuti stars appears to be diverse.

In the context of solar-like pulsations, $\nu_{\rm max}$ is generally linked to the granulation timescale, which is associated with stellar surface convection. Envelopes of solar-like oscillators are convective, δ Scutis possess dominantly radiative envelopes accompanied by a very thin surface-convective layer. Thus some form of surface turbulence may be expected in these stars, which may be responsible for the observed correlation between their $\nu_{\rm max}$ and $\Delta\nu$. The latter, in both classes of pulsators, is proportional to the mean stellar density, and hence is representative of their evolutionary conditions.

2.6. *Relationship between $\nu_{\rm max}$ and gross stellar properties*

The frequency at which the Sun's oscillation power peaks is $\nu_{\rm max} \sim 3$mHz. This may be seen as a balance between mode inertia and near-surface attenuation of wave energy. Modes with low frequency have low visibility at the photosphere because their mode inertia is high, whereas higher frequency modes have larger surface visibility. It naturally causes higher-frequency modes to be more visible than their low-frequency counterparts. Modes with frequencies closer to or higher than the solar acoustic cutoff (~ 5.5 mHz) are likely to increasingly tunnel out into the atmosphere, and hence, do not reflect from the surface to form standing waves, which are observed as eigenmodes. Additionally, non-adiabatic effects result in wave dissipation, which causes observed mode power to fall with frequency. These effects compete with each other and an intermediate frequency becomes the $\nu_{\rm max}$ at which mode power peaks. However, this is a case where turbulent processes stochastically excite the oscillations.

In contrast, modes in δ Scutis are driven by the κ (opacity) mechanism, which results in unpredictable mode amplitudes. Thus $\nu_{\rm max}$ is ostensibly less meaningful in δ Scutis than in stars with substantial outer convection zones. However, the present results (Figure 3b) show that $\nu_{\rm max}$ scales surprisingly tightly with the acoustic cutoff frequency ($\propto g\,T_{\rm eff}^{-0.5}$), vindicating what was suggested by Brown et al. (1991). A likely implication is that amplitudes are assigned non-randomly in δ Scutis, although exactly how or why remain unclear. Building a sample of massive stars to test this hypothesis forms a future goal for us.

The appearance of $\nu_{\rm max}$ in solar-like stars is a consequence of the interplay between reduced mode visibility at lower frequencies (due to increasing mode-inertia) and damping of higher frequency modes caused by near-surface turbulence and non-adiabatic effects. An intermediate mode ($\sim \nu_{\rm max}$) thus gains the largest power, for which these effects balance each other. The occurrence of a $\nu_{\rm max}$ in δ Scuti stars, among samples that display regularly spaced oscillations, is not quite as easy to explain. One possibility is that it may be conceived in a similar framework, with the only exception that damping of the high-frequency modes may be due to non-adiabatic radiative processes (Houdek et al. 1999) such as radiative diffusion. As discussed in Zwintz, K. et al. (2011), the outer layers of the partial He II ionization zone, where opacity reduces radially outward, contribute to mode damping. Whereas, the inner regions, where opacity increases outward, leads to mode excitation. Simulations of acoustic modes (Samadi, R. et al. 2002, figure 1) have shown the damping rates of p-modes to be increasing with oscillation frequency, in the range of 0.2-0.6 mHz ($\sim$ 17-52 d^{-1}).

3. DISCUSSION

Gaia DR3 provides various stellar parameters for a large number of δ Scutis. In this study, we intend to assess whether the evolutionary stage of a δ Scuti star can be estimated given the $\nu_{\rm max}$ of its acoustic oscillation. The $\nu_{\rm max} - \varepsilon$ mapping may prove useful for the asteroseismic determination of the evolutionary stages of new δ Scutis whose oscillations will be measured by the Plato instrument. Figure 1(a) indicates that a star having $\nu_{\rm max} > 30\mathrm{d}^{-1}$ exclusively belongs to Group-2 and its evolutionary phase may be uniquely determined from

$$\varepsilon = 379.614 - 5.83\ (\nu_{\rm max}/\mathrm{d}^{-1}),$$

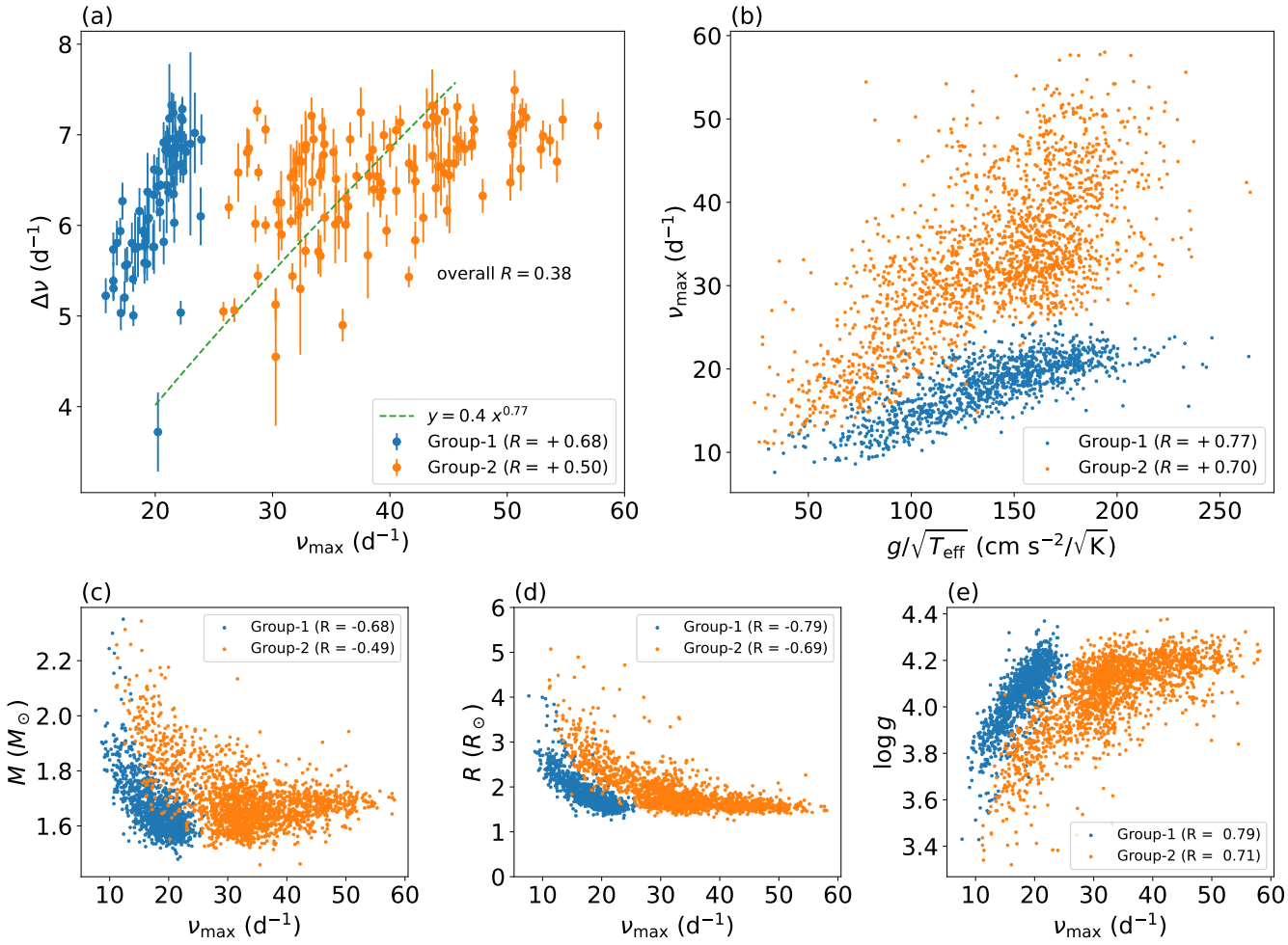

Figure 3. (a) Large frequency separation ($\Delta\nu$) as a function of ν_{max} for 400 stars having both measurements available. Stars are color-coded according to their assigned Groups in Figure 1. Although a weak correlation ($R = 0.38$) does not indicate a strong dependence between the two quantities for the entire sample, stars in Group-1 comparatively exhibit a more constricted variation. The dashed line marks the $\delta\nu - \nu_{max}$ trend observed in surface convection-driven solar-like oscillations. (b) ν_{max} as a function of $g/\sqrt{T_{eff}}$, which is a proxy of acoustic cut-off frequency that limits the upper bound of visible modes in Solar-like oscillators. A correlation is also visible here for δ Scuti stars. Following figures show the connections between ν_{max} and other structural parameters – (c) mass, (d) radius, and (e) log g.

although with larger uncertainty. Because stars with $\nu_{max} < 30 d^{-1}$ may either belong to Groups 1 or 2, their evolutionary phases also cannot be tightly constrained. As a consequence of the self-intersecting nature of the evolutionary tracks (Murphy et al. 2021, Fig.12), δ Suctis often exhibit similar luminosity, T_{eff}, and even comparable oscillation frequencies (Murphy et al. 2021, Fig.11) during both pre-main sequence and main-sequence phases, thus limiting asteroseismic methods from distinguishing between degenerate solutions for stellar ages. Therefore, the pulsation characteristics, e.g., ν_{max} (and hence A_{max}) do not presently appear to provide tight constrains on the ages of δ Scuti stars. Oscillation phases of the strongest amplitude modes, in conjunction with the ν_{max} and A_{max}, may provide better information about evolutionary phases.

Unlike other pulsators, the asteroseismic properties of δ Scutis do not exhibit sharp correlations with other stellar parameters (Bedding et al. 2023; Balona 2024) including structure, spectroscopic, or photometric properties. The primary reason may be the spread in rotation (García Hernández et al. 2022) and possibly the inclination angle, which may significantly broaden the dependencies between various quantities, obscuring the true correlations. With the sheer number of δ Scutis observed by NASA's TESS space telescope, correlations involving several asteroseismic parameters are expected to appear when stellar properties are investigated on an ensemble scale. While rotation can perturb both the

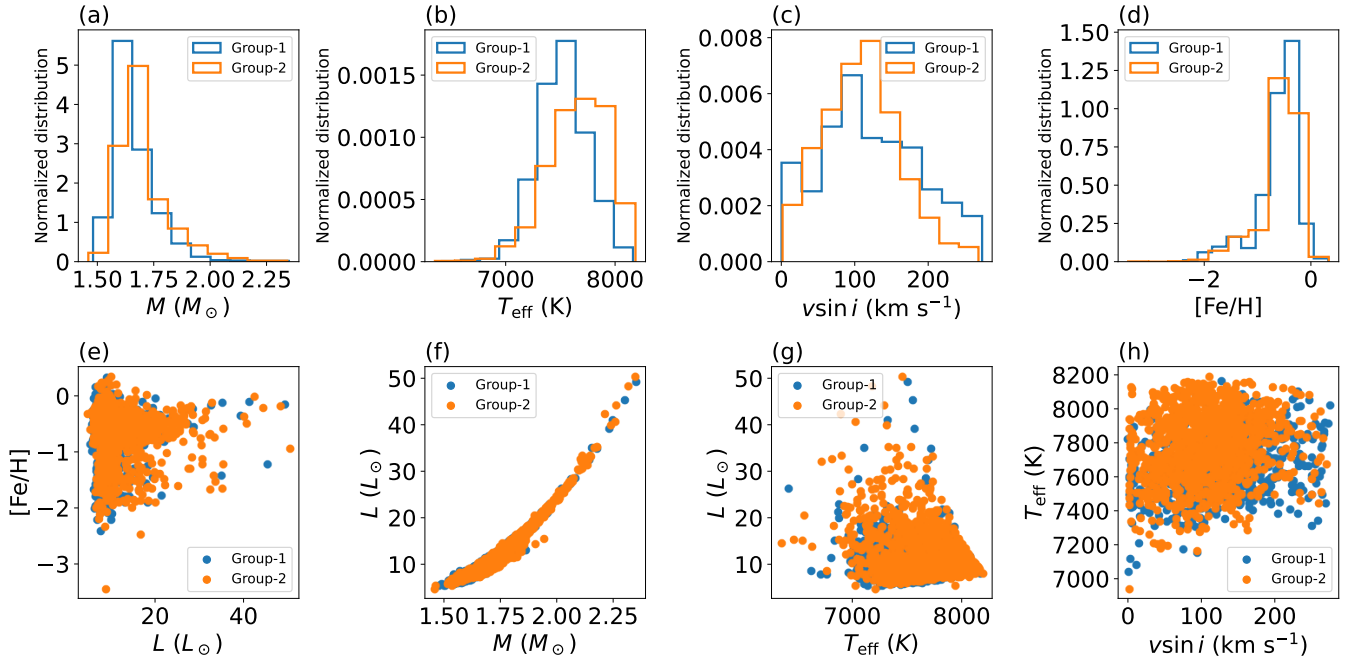

Figure 4. (*top*) Comparing the parameter-statistics between the Groups of stars for (a) mass, (b) effective temperature $T_{\rm eff}$, (c) projected rotational velocity $v \sin i$, and (d) metallicity [Fe/H]. The figures indicate very high degree of similarity among the statistics of each Group. (*bottom*) Demonstrating the dependence between various observables, color coded according to the Groups of the stars: (e) luminosity-metallicity, (f) mass-luminosity, (g) effective temperature-luminosity, and (h) $T_{\rm eff}$-rotational velocity. The figure conveys that these Groups are not distinguishable based on their non-seismic properties.

pulsation frequency and amplitude, inclination angle can only affect the latter. Therefore, in principle, the excess spread in the $(\nu_{\rm max} - \varepsilon)$ relation (Fig. 1a) may be possibly used to constrain stellar rotation first, which in turn can help in extracting the inclination angle from the observationally acquired $v \sin i$, if stellar radius R is known. If the rotation-inclination contributions to the correlation spreads can be quantified, it may even offer ways to estimate rotation rates from the $\nu_{\rm max} - A_{\rm max}$ relation (Fig. 1b). Although we are unable to attempt these inferences at present, asteroseismology seems capable of constraining rotation, inclination angle, evolutionary phase, and ages of δ Scuti stars.

The strong correlations between $\nu_{\rm max}, \nu_{\rm 2max}$ and and $\Delta\nu$ and other stellar properties suggest that mode amplitudes are set non-randomly and contain potentially important a meaningful quantity for δ Scutis. This finding was made possible because of the availability of high-quality photometric data provided by the TESS mission, allowing us to identify and build a large catalogue of δ Scutis.

APPENDIX

A. DISTINGUISHING BETWEEN THE GROUPS

The classification of the stars into the Groups was entirely based on their seismic properties (i.e., $\nu_{\rm max}$). In order to understand the detailed functioning of these stars, it is imperative to analyze how they differ in terms of their physical properties. We were unable to find non-seismic characteristics (e.g., mass, metallicity, radius, $v \sin i$ etc.) which may be used to distinguish between these groups. In the top row of Figure 4, we compare the distributions of different parameters across the Groups and found that they are similar to a significant extent. In the bottom row of Figure 4, we plot the dependence between various observables of these stars and also noticed that the Groups do not occupy distinct positions in the analyzed phase space.

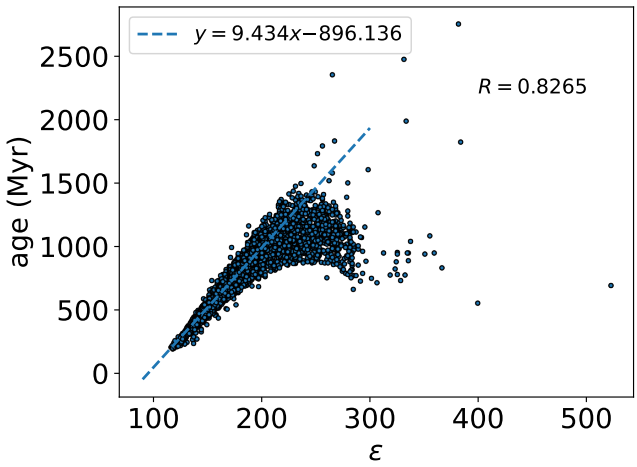

Figure 5. Ages (in Myr) of δ Scutis shown as a function of their evolutionary stages, displaying a high degree of correlation. The dashed line corresponds to the best fit obtained from the linear regime. We extrapolate this line to convey that some of the stars have reached their evolutionary stages at ages younger than expected.

B. LINKING AGE WITH EVOLUTIONARY STAGE

Gaia DR3 measurements of ages were available for select stars in our sample. Although stellar ages are not directly connected to evolutionary stages, they find applications in the studies of star formation and galactic evolution. Age and evolutionary phase are strongly correlated ($R = 0.8$), as we show in Figure 5. Stellar ages monotonically increase with evolutionary stages until $\varepsilon \lesssim 200$, beyond which a non-linear variation starts appearing. Thus, a one-to-one correspondence between ε and age cannot always be drawn. For instance, two stars at the same age of ~ 750 Myr could be passing through different evolutionary stages, e.g., $\varepsilon \sim 200$ and 300. Nevertheless, below ages of ~ 750 Myr, evolutionary stages may be uniquely determined, and we obtained a relation

$$\text{age (Myr)} = 9.434\varepsilon - 896.136$$

by fitting this regime with a linear function. The non-linear regime appears because of a number of stars evolve faster than anticipated, arriving at their present evolutionary phases earlier than the timescale estimated from the linear regime. The transition from linear to non-linear phase occurs around $\varepsilon \sim 250$. Since Hidalgo et al. (2018) refers to $\varepsilon = 300$ as corresponding to the main sequence at a core-Hydrogen abundance level of $X_c = 0.3$, the aforementioned transition may be occurring somewhere before this stage.

C. EVOLUTIONARY CHANGES IN ASTEROSEISMIC ATTRIBUTES

Young δ Scutis pulsate with high frequencies (Bedding et al. 2020), and perhaps spin faster, with $v \sin i$ reaching hundreds of km s^{-1} in some cases. In contrast, high-amplitude δ Scuti (HADS, Balona 2016) stars are more evolved slowly rotating objects, showing relatively high amplitude pulsations primarily in the fundamental radial mode. These two observational findings may be unified with the interpretation that stars grow larger with evolution and therefore pulsate with modes of decreasing frequency and increasing amplitude. To provide a clear picture of the time-dependent changes in asteroseismic characteristics, we show in Figure 6 a stack of pulsation spectra of 40 arbitrarily chosen δ Scutis, along with their evolutionary stages ε and $A_{\rm max}$, sorted in the descending order of $\nu_{\rm max}$. We see a rough trend - ε and $A_{\rm max}$ appear to increase with decreasing $\nu_{\rm max}$. Stacked pulsation spectra (Barac et al. 2022; Bedding et al. 2023; Read et al. 2024; Hey, Daniel & Aerts, Conny 2024) have turned into an useful tool for gaining valuable insights into the evolutionary properties of stars.

Acknowledgments: We have made use of the SIMBAD and VizieR databases, operated at CDS, Strasbourg, France. We also acknowledge the data provided by the Space Telescope Science Institute's MAST database based on the observations from the TESS mission, funded by the NASA's Science Mission Directorate. Data from the European Space Agency's Gaia mission (https://www.cosmos.esa.int/gaia), processed by the Gaia Data Processing and Analysis

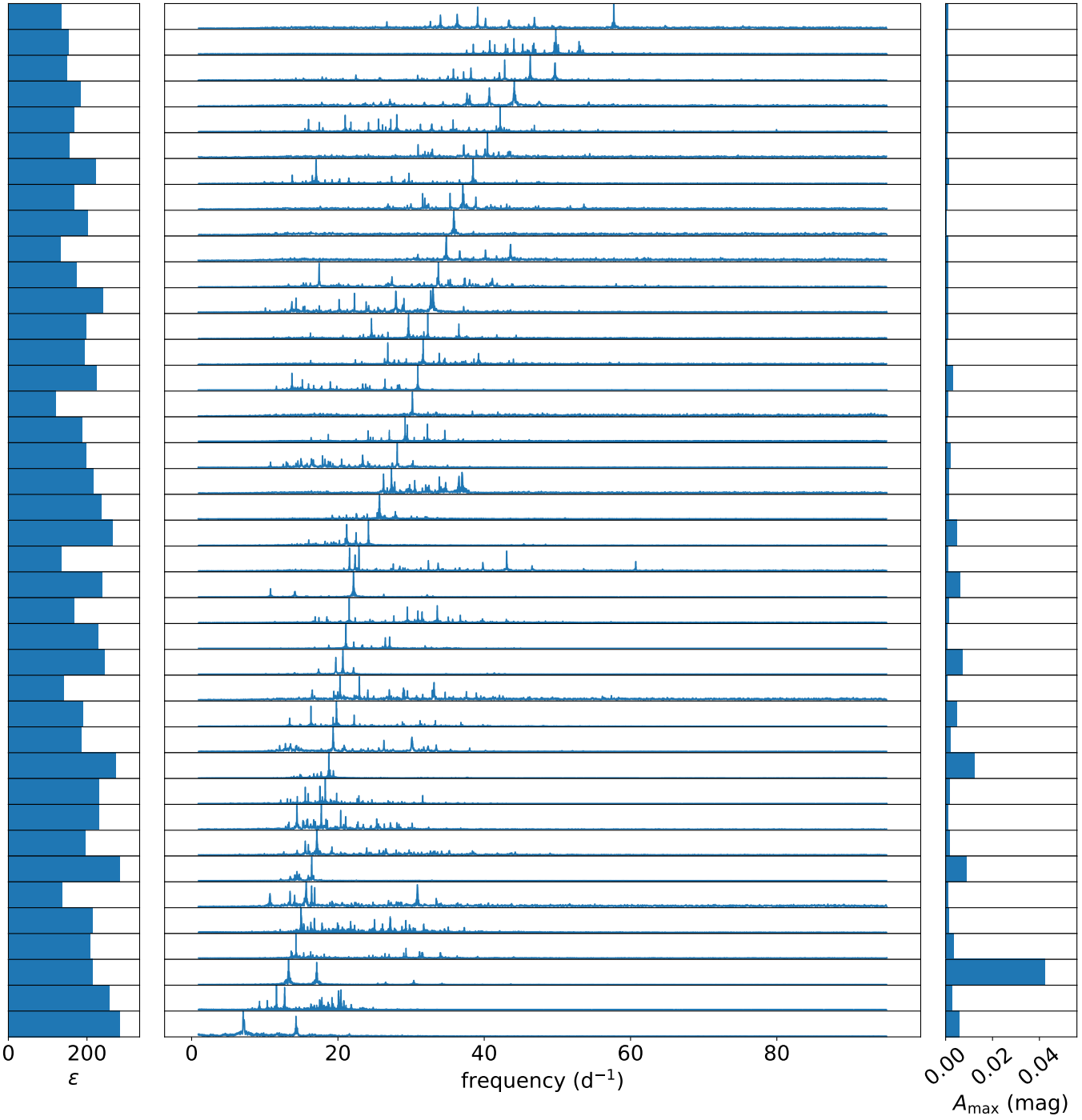

Figure 6. Demonstrating evolutionary changes in the asteroseismic properties of 40 arbitrarily selected stars from our sample. (*Middle*) Oscillation spectra are arranged in descending order of $\nu_{\rm max}$. For stars corresponding to each power spectrum shown in the middle, we plot horizontal levels proportional to their (*Left*) evolutionary stages ε and (*Right*) strongest pulsation amplitudes $A_{\rm max}$. On average, ε shows a tendency of increasing downward, implying stars in this diagram evolve from top to bottom, with decreasing $\nu_{\rm max}$ and growing $A_{\rm max}$.

Consortium (DPAC), has been useful for our analysis. We have used `NumPy` (van der Walt et al. 2011), `SciPy` (Oliphant 2007), and `Matplotlib` (Hunter 2007) like Python Packages in this work. The `Lightkurve` (Lightkurve Collaboration 2018) Package has been used for constructing Stellar oscillation spectra. The MCMC fittings have been carried out using the code `Dynesty` (Speagle 2020). Most of the computations have been carried out in the Intel Lab Academic Compute Environment. We acknowledge support from the DAE, Government of India (grant no. RTI 4002). This research was supported in part by a generous donation (from the Murty Trust) aimed at enabling advances in astrophysics through the use of machine learning. Murty Trust, an initiative of the Murty Foundation, is a not-for-profit organisation dedicated to the preservation and celebration of culture, science, and knowledge systems born out of India. The Murty Trust is headed by Mrs. Sudha Murty and Mr. Rohan Murty. We are grateful to the referees for providing constructive comments.

REFERENCES

Aerts, C. 2021, Rev. Mod. Phys., 93, 015001, doi: 10.1103/RevModPhys.93.015001

Baglin, A., Breger, M., Chevalier, C., et al. 1973, A&A, 23, 221. https://ui.adsabs.harvard.edu/abs/1973A&A....23..221B

Balona, L. A. 2016, Monthly Notices of the Royal Astronomical Society, 459, 1097, doi: 10.1093/mnras/stw671

—. 2024, The Open Journal of Astrophysics, 7, doi: 10.21105/astro.2109.12574

Balona, L. A., & Dziembowski, W. A. 2011, Monthly Notices of the Royal Astronomical Society, 417, 591, doi: 10.1111/j.1365-2966.2011.19301.x

Balona, L. A., Joshi, S., Joshi, Y. C., & Sagar, R. 2012, Monthly Notices of the Royal Astronomical Society, 429, 1466, doi: 10.1093/mnras/sts429

Barac, N., Bedding, T. R., Murphy, S. J., & Hey, D. R. 2022, Monthly Notices of the Royal Astronomical Society, 516, 2080, doi: 10.1093/mnras/stac2132

Barceló Forteza, S., Roca Cortés, T., & García, R. A. 2018, Astronomy & Astrophysics, 614, A46, doi: 10.1051/0004-6361/201731803

Barceló Forteza, S., Roca Cortés, T., García Hernández, A., & García, R. A. 2017, A&A, 601, A57, doi: 10.1051/0004-6361/201628675

Bedding, T. R., Murphy, S. J., Hey, D. R., et al. 2020, Nature, 581, 147, doi: 10.1038/s41586-020-2226-8

Bedding, T. R., Murphy, S. J., Crawford, C., et al. 2023, The Astrophysical Journal Letters, 946, L10, doi: 10.3847/2041-8213/acc17a

Borucki, W. J., Koch, D., Basri, G., et al. 2010, Science, 327, 977, doi: 10.1126/science.1185402

Bowman, D. M. 2020, Frontiers in Astronomy and Space Sciences, 7, doi: 10.3389/fspas.2020.578584

Bowman, D. M., Kurtz, D. W., Breger, M., Murphy, S. J., & Holdsworth, D. L. 2016, Monthly Notices of the Royal Astronomical Society, 460, 1970, doi: 10.1093/mnras/stw1153

Breger, M. 1982, PASP, 94, 845, doi: 10.1086/131074

Brito, A., & Lopes, I. 2021, Monthly Notices of the Royal Astronomical Society, 507, 5747, doi: 10.1093/mnras/stab2501

Brown, T. M., Gilliland, R. L., Noyes, R. W., & Ramsey, L. W. 1991, ApJ, 368, 599, doi: 10.1086/169725

Chevalier, C. 1971, A&A, 14, 24. https://ui.adsabs.harvard.edu/abs/1971A&A....14...24C

Córsico, A. H. 2020, Frontiers in Astronomy and Space Sciences, 7, doi: 10.3389/fspas.2020.00047

Daszyńska-Daszkiewicz, J., Dziembowski, W. A., Pamyatnykh, A. A., & Goupil, M.-J. 2002, A&A, 392, 151, doi: 10.1051/0004-6361:20020911

Fouesneau, M., Frémat, Y., Andrae, R., et al. 2023, A&A, 674, A28, doi: 10.1051/0004-6361/202243919

Gaia Collaboration, De Ridder, J., Ripepi, V., et al. 2023, A&A, 674, A36, doi: 10.1051/0004-6361/202243767

García Hernández, A., Pascual-Granado, J., Lares-Martiz, M., et al. 2022, Proceedings of the International Astronomical Union, 18, 239–249, doi: 10.1017/S1743921323003368

Gough, D. O. 1986, in Hydrodynamic and Magnetodynamic Problems in the Sun and Stars, ed. Y. Osaki, 117. https://ui.adsabs.harvard.edu/abs/1986hmps.conf..117G

Handler, G. 2009, AIP Conference Proceedings, 1170, 403, doi: 10.1063/1.3246528

Hey, Daniel, & Aerts, Conny. 2024, A&A, 688, A93, doi: 10.1051/0004-6361/202450489

Hidalgo, S. L., Pietrinferni, A., Cassisi, S., et al. 2018, The Astrophysical Journal, 856, 125, doi: 10.3847/1538-4357/aab158

Houdek, G., Balmforth, N., Christensen-Dalsgaard, J., & Gough, D. 1999, Astron. Astrophys., 351, doi: 10.48550/arXiv.astro-ph/9909107

Howell, S. B., Sobeck, C., Haas, M., et al. 2014, PASP, 126, 398, doi: 10.1086/676406

Hunter, J. D. 2007, Computing in Science & Engineering, 9, 90, doi: 10.1109/MCSE.2007.55

Lightkurve Collaboration. 2018, Lightkurve: Kepler and TESS time series analysis in Python, Astrophysics Source Code Library. http://ascl.net/1812.013

Mermilliod, J. C., Mathieu, R. D., Latham, D. W., & Mayor, M. 1998, A&A, 339, 423. https://ui.adsabs.harvard.edu/abs/1998A&A...339..423M

Murphy, S. J., Joyce, M., Bedding, T. R., White, T. R., & Kama, M. 2021, Monthly Notices of the Royal Astronomical Society, 502, 1633, doi: 10.1093/mnras/stab144

Oliphant, T. E. 2007, Computing in Science & Engineering, 9, 10, doi: 10.1109/MCSE.2007.58

Pedregosa, F., Varoquaux, G., Gramfort, A., et al. 2011, Journal of Machine Learning Research, 12, 2825. https://scikit-learn.org/

Read, A. K., Bedding, T. R., Mani, P., et al. 2024, Monthly Notices of the Royal Astronomical Society, 528, 2464, doi: 10.1093/mnras/stae165

Reese, D. R., Prat, V., Barban, C., van 't Veer-Menneret, C., & MacGregor, K. B. 2013, A&A, 550, A77, doi: 10.1051/0004-6361/201220506

Ricker, G. R., Winn, J. N., Vanderspek, R., et al. 2014, Journal of Astronomical Telescopes, Instruments, and Systems, 1, 014003, doi: 10.1117/1.JATIS.1.1.014003

Royer, F., Zorec, J., & Gómez, A. E. 2007, A&A, 463, 671, doi: 10.1051/0004-6361:20065224

Samadi, R., Goupil, M.-J., & Houdek, G. 2002, A&A, 395, 563, doi: 10.1051/0004-6361:20021322

Speagle, J. S. 2020, Monthly Notices of the Royal Astronomical Society, 493, 3132–3158, doi: 10.1093/mnras/staa278

Sreenivas, K. R., Bedding, T. R., Li, Y., et al. 2024, Monthly Notices of the Royal Astronomical Society, 530, 3477, doi: 10.1093/mnras/stae991

Stello, D., Cantiello, M., Fuller, J., et al. 2016, Nature, 529, 364–367, doi: 10.1038/nature16171

Suárez, J.-C., Michel, E., Pérez Hernández, F., et al. 2002, A&A, 390, 523, doi: 10.1051/0004-6361:20020565

Uytterhoeven, K., Moya, A., Grigahcène, A., et al. 2011, A&A, 534, A125, doi: 10.1051/0004-6361/201117368

van der Walt, S., Colbert, S. C., & Varoquaux, G. 2011, Computing in Science & Engineering, 13, 22, doi: 10.1109/MCSE.2011.37

Ziaali, E., Bedding, T. R., Murphy, S. J., Van Reeth, T., & Hey, D. R. 2019, Monthly Notices of the Royal Astronomical Society, 486, 4348, doi: 10.1093/mnras/stz1110

Zwintz, K., & Steindl, T. 2022, Frontiers in Astronomy and Space Sciences, 9, doi: 10.3389/fspas.2022.914738

Zwintz, K., Lenz, P., Breger, M., et al. 2011, A&A, 533, A133, doi: 10.1051/0004-6361/201117272